

OPEN

Differentiation of Small Hepatic Abscess From Hepatic Metastasis With a Combination of Imaging Parameters

Chul-min Lee, MD, Bo-Kyeong Kang, MD, PhD, and Mimi Kim, MD, PhD

Objective: We aimed to evaluate the diagnostic performance of the combination imaging features to differentiate small (the lesion size of 3 cm or less) hepatic abscess from metastasis.

Methods: This retrospective study included patients with preexisting malignancy and small hepatic lesions who underwent contrast-enhanced computed tomography (CT) and gadolinic acid-enhanced magnetic resonance imaging (MRI) within 4 days between March 2017 and July 2020. Two radiologists independently evaluated the imaging features of each focal hepatic lesion. Laboratory parameters were also recorded. Significant parameters differentiating hepatic abscess from hepatic metastasis were identified by univariate generalized estimating equation regression. We compared the diagnostic performances of laboratory parameters, imaging features, and their combinations.

Results: We included 16 patients (10 males and 6 females) with 35 hepatic abscesses and 21 patients (13 males and 8 females) with 62 metastases with a mean age of 70.3 years in this study. Abnormal segmental neutrophil, pathy parenchymal enhancement on CT, and absence of dark rim on MRI were associated with hepatic abscess (all $P < 0.01$). The combination of CT and MRI parameters showed significantly higher specificity and positive predictive value than CT alone ($P \leq 0.031$), without significant difference in sensitivity and negative predictive value.

Conclusions: We have demonstrated that the combination of CT and MRI imaging features is helpful for the differentiation of small hepatic abscess from metastasis.

Key Words: computed tomography, liver abscess, magnetic resonance imaging, metastasis

(*J Comput Assist Tomogr* 2022;46: 514–522)

Hepatic metastasis is the most common malignant lesion in the liver and typical imaging features have been extensively evaluated in previous studies.^{1–4} On the other hand, hepatic abscess is a localized collection of necrotic inflammatory material caused by bacterial, fungal, and parasitic infections. Typical imaging features of a hepatic abscess include cluster sign and double target sign on computed tomography (CT) and magnetic resonance imaging (MRI).^{2,5,6}

It is known that the patients with preexisting malignancy are prone to develop hepatic abscess or metastasis. However, the 2 diseases have different managements and prognoses. The imaging

features of hepatic abscess and metastasis are often difficult to distinguish because a hepatic abscess can show nonspecific imaging features according to maturity. There are overlapping image features between the 2 diseases, such as peripheral rim enhancement and diffusion restriction, and small hepatic abscess often does not show typical imaging features.^{2,3,7} In addition, the targeted biopsy is an invasive procedure and often difficult for small lesions. The differentiation between the 2 diseases is also difficult in other modalities, such as positron emission tomography.⁸

Magnetic resonance imaging is performed not only to detect hepatic metastasis not seen on CT but also to evaluate the indeterminate hepatic lesions observed on CT. Several studies have reported imaging features that distinguish hepatic abscess from metastasis on CT or MRI alone.^{1–4,7} However, no research evaluated the diagnostic performance of the combination of CT and MRI imaging features with laboratory parameters for differentiation of small hepatic abscess from metastasis.

Therefore, the purpose of our study was to evaluate the diagnostic performances of the laboratory, CT and MRI imaging features, and their combinations for the differentiation of small hepatic abscess from metastasis in patients with preexisting malignancy.

MATERIALS AND METHODS

This study was approved by the institutional review board of our institution, which waived the requirement for informed consent because of the retrospective nature of this study.

Study Population

We retrospectively included patients who underwent contrast-enhanced CT and gadolinic acid-enhanced MRI to differentiate hepatic abscess from metastasis at our institution between March 2017 and July 2020. The inclusion criteria were as follows: (1) focal hepatic lesion ≤ 3 cm on both CT and MRI (up to 5 lesions per patient) and (2) within 4 days interval between CT and MRI examination. The exclusion criteria were as follows: (1) lesion size > 3 cm, (2) lesion with highly suggestive imaging features of the hepatic abscess (ie, cluster sign or target sign), (3) loss of follow-up without pathological confirmation or clinical diagnosis, and (4) inadequate image quality for interpretation, such as lack of sequence or artifact. In addition, the following laboratory findings at the time of CT examination were recorded through the electrical medical record review: white blood cell and percentage of segment neutrophil, total and direct bilirubin, and C-reactive protein (CRP). At our institution, the abnormal range of white blood cell is less than 4000/mm³ or more than 10,000/mm³, abnormal percentage of segmental neutrophil is less than 50% or more than 75%, and elevated total bilirubin, direct bilirubin, and CRP is higher than 1.2 mg/dL, 0.19 mg/dL, and 0.5 mg/dL, respectively. We also evaluated each patient's underlying preexisting malignancy and history of cancer operation.

We would note that, in our institution, patients suspected of infection in consideration of both imaging findings and clinical

From the Department of Radiology, Hanyang University School of Medicine, Hanyang University Medical Center, Seoul, Korea.

Received for publication July 19, 2021; accepted December 31, 2021.

Correspondence to: Mimi Kim, MD, PhD, Department of Radiology, Hanyang University Seoul Hospital, Hanyang University, 222-1, Wangsimni-ro, Seongdong-gu, Seoul, 04763, Republic of Korea (e-mail: bluefish010@naver.com).

The authors declare no conflict of interest.

Copyright © 2022 The Author(s). Published by Wolters Kluwer Health, Inc. This is an open-access article distributed under the terms of the Creative Commons Attribution-Non Commercial-No Derivatives License 4.0 (CCBY-NC-ND), where it is permissible to download and share the work provided it is properly cited. The work cannot be changed in any way or used commercially without permission from the journal.

DOI: 10.1097/RCT.0000000000001307

presentations are supposed to stop chemotherapy and treat the infection first. Therefore, patients with hepatic abscesses are not treated simultaneously with antibiotics and chemotherapy. If there was no improvement with sufficient antibiotic treatment, hepatic metastasis was considered, and then chemotherapy was performed.

CT Examination

Patients underwent CT using 64-detector row CT systems (Somatom Definition Edge and Somatom Definition FLASH [Siemens Healthineers, Erlangen, Germany]; Brilliance 64 [GE Healthcare, Chicago, IL]). Unenhanced, arterial phase (AP; determined using bolus triggering method), portal venous phase (PP; 70 seconds), and delayed phase (3 minutes) dynamic contrast-enhanced images in the axial plane with 3-mm thickness and coronal reconstruction of portal phase image with 3-mm thickness were obtained in all patients after intravenous iodine contrast injection of 120 to 150 mL of iohexol (Bonorex, Central Medical Service) at a rate of 3 mL/s using a power injector.

MRI Examination

All patients underwent MRI after CT scans on a 3.0-T scanner (Ingenia or Achieva, Philips Medical Systems). Unenhanced MRI included T1-weighted dual gradient-echo in- and opposed-phase imaging, T2-weighted navigator-triggered turbo spin-echo imaging, and diffusion-weighted single-shot spin-echo echo-planar imaging. Gadoxetate disodium-enhanced imaging was performed using a bolus injection of 0.025 mmol/kg gadoxetate disodium at a rate of 1.0 mL/s followed by a subsequent 20 mL of saline flush delivered using a power injector. T1-weighted 3-dimensional gradient-echo imaging was obtained before contrast injection and in the AP (5 seconds after peak aortic enhancement determined using a 1.0 mL test bolus injection), PP (50 seconds), transitional phase (TP; 3 minutes), and hepatobiliary phase (HBP; 20 minutes) after contrast enhancement.

Image Analysis

All CT and MR images were independently reviewed by 2 board-certified abdominal radiologists (M.K and C.-m.L, each with >6 years of experience in hepatic imaging) on a picture archiving and communication system. Both readers were blinded

to the final diagnosis of each focal hepatic lesion, except for the alternative diagnosis of hepatic abscess or metastasis. After an independent review by both readers, a consensus was reached for the discordant cases.

On CT examination, the following imaging features were analyzed for each focal hepatic lesion: (a) size and size discrepancy, (b) density, (c) rim enhancement in AP and PP, (d) perilesional enhancement in AP, (e) patchy parenchymal enhancement in AP, and (f) bile duct dilatation. In addition, the following imaging features were evaluated on MRI: (a) size and size discrepancy; (b) signal intensity (SI); (c) margin; (d) rim enhancement in AP, PP, and TP; (e) perilesional enhancement in AP; (f) patchy parenchymal enhancement in AP; (g) presence of dark rim and perilesional low SI in HBP; and (h) diffusion restriction pattern in diffusion-weighted image (DWI). Detailed definitions and descriptions of each imaging feature are summarized in Supplementary Table 1.

Reference Standard

Focal hepatic lesions were histopathologically confirmed by biopsy or surgery. If there was no histopathologic confirmation, it was clinically diagnosed as hepatic abscess when improved during follow-up with antibiotics. In contrast, it was diagnosed as hepatic metastasis if there was an improvement after chemotherapy or progression on follow-up imaging examinations.

Statistical Analysis

We performed a per-lesion analysis to identify significant imaging features for the differentiation of hepatic abscesses from metastasis. The differences in the CT and MR imaging features were evaluated using the χ^2 test. We performed univariate generalized estimating equation (GEE) regression to identify significant imaging features and laboratory parameters differentiating hepatic abscess from metastasis. The diagnostic performances of each parameter and their combination were calculated as sensitivity, specificity, positive predictive value (PPV), negative predictive value (NPV), and diagnostic accuracy and were compared using the McNemar test. Interobserver agreement for each imaging feature was evaluated using κ statistics for the presence of imaging features and intraclass correlation coefficient for the size. They were interpreted as follows: 0.00 to 0.20, poor; 0.21 to 0.40, fair; 0.41 to 0.60, moderate; 0.61 to 0.80, good; and 0.81 to 1.00, excellent

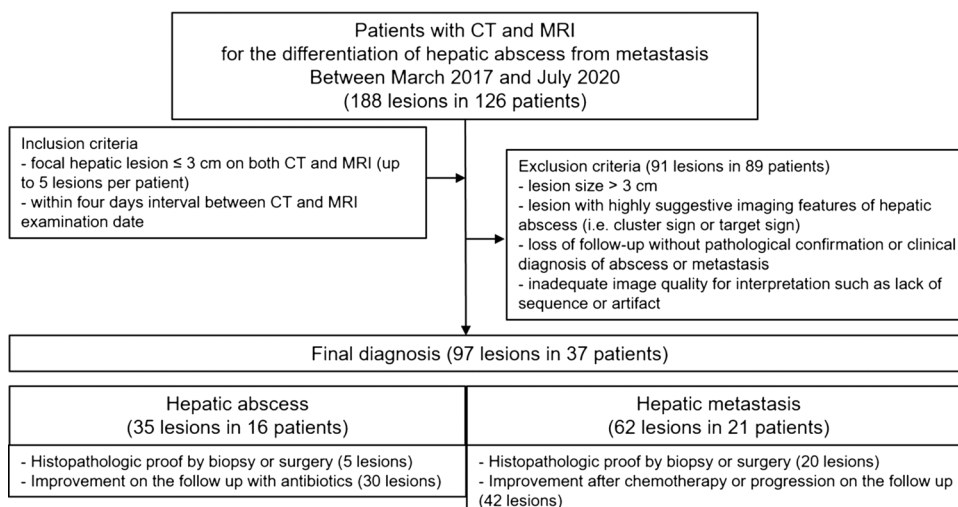


FIGURE 1. Flow chart of the study population.

agreement. A *P* value of <0.05 was considered statistically significant. Statistical analysis was performed using SPSS version 26.0 statistical software (IBM, Armonk, NY).

RESULTS

Patient Characteristics

There were 23 men and 14 women with a mean age of 70.3 years (range, 21–92 years). Thirty-five hepatic abscesses in 16 patients and 62 metastases in 21 patients were analyzed in the study. Of the 35 hepatic abscesses, 5 lesions (14.3%) were pathologically confirmed by biopsy or surgery, and 30 lesions (85.7%) were diagnosed as hepatic abscesses owing to improvement in the follow-up with antibiotics. Among 62 hepatic metastases, 20 lesions (32.3%) were histopathologically confirmed after biopsy or surgery. The remaining 42 lesions (67.7%) were clinically diagnosed as metastases owing to improvement after chemotherapy or progression on follow-up imaging studies (Fig. 1).

Table 1 summarizes the characteristics of the study population. Of the 16 patients with hepatic abscess, 12 patients (75%) had a single lesion, and 4 patients (25%) had 2 or more lesions. Among 21 patients with hepatic metastasis, 9 patients (42.9%) had a single lesion, and 12 patients (57.1%) had 2 or more lesions.

Eleven patients (11 of 16 [68.9%]) with hepatic abscess showed abnormal segment neutrophil, making a significant difference between the 2 groups ($P = 0.006$). Pancreatic cancer (8 of 21 [38.1%]) was the most common preexisting malignancy in cases of hepatic metastasis, followed by colon cancer (6 of 21 [28.6%]). In contrast, hepatobiliary cancer (9 of 16 [56.3%]) was the most common in hepatic abscess, and gastric cancer was the second most common (4 of 16 [25%]).

Significant Imaging Features for the Differentiation of Hepatic Abscess From Metastasis

Perilesional enhancement and patchy parenchymal enhancement in AP, rim enhancement in PP, and presence of bile duct dilatation showed significant differences between hepatic abscess and metastasis on CT ($P \leq 0.005$), which were more frequently seen in hepatic abscesses than metastasis except for bile duct dilatation. There were significant differences in the margin, perilesional enhancement and patchy parenchymal enhancement in AP, dark rim and perilesional low SI in HBP, DWI pattern, and size discrepancies (T1-weighted images-HBP and T1-weighted images-T2-weighted images) between hepatic abscess and metastasis on MRI ($P \leq 0.017$). Ill-defined margin, absence of dark rim, perilesional low SI in HBP, central hyperintensity in

TABLE 1. Baseline Demographics and Clinical Characteristics of the Patients

	Abscess (n = 16)	Metastasis (n = 21)	<i>P</i>
Age, y*	72.1 ± 18.2 (21–92)	67.9 ± 10.3 (37–81)	0.372
Sex, n (%)			
Male	10 (62.5)	13 (61.9)	
Female	6 (37.5)	8 (38.1)	
WBC, 10 ³ /mm ³ *	10.7 ± 6.6	7.2 ± 4.4	0.085
Abnormal WBC	9 (56.3)	8 (38.1)	0.272
Segment neutrophil*	72.2 ± 23.3	65.2 ± 10.2	0.278
Abnormal segment neutrophil	11 (68.8)	4 (19.0)	0.006
CRP, mg/dL*	13.9 ± 14.2	6.8 ± 7.3	0.116
CRP elevation	15 (93.8)	13 (61.9)	0.050
Total bilirubin, mg/dL*	3.3 ± 5.9	1.9 ± 2.3	0.337
Total bilirubin elevation	8 (50.0)	6 (28.6)	0.183
Direct bilirubin, mg/dL*	2.1 ± 4.2	1.1 ± 1.7	0.464
Direct bilirubin elevation	12 (75.0)	7 (33.3)	0.020
No. lesions			0.183
Single	12 (75.0)	9 (42.9)	
Multiple	4 (25.0)	12 (57.1)	
Underlying preexisting malignancy			—
Hepatobiliary cancer†	9 (56.3)	2 (9.5)	
Pancreatic cancer‡	1 (6.3)	8 (38.1)	
Colon cancer	0	6 (28.6)	
Gastric cancer	4 (25.0)	0	
Breast cancer	0	1 (4.8)	
Other or unknown primary cancer	2 (12.5)	4 (19.0)	
History of cancer operation			1.000
Absent	13 (81.3)	16 (76.2)	
Present	3 (18.8)	5 (23.8)	

Data are presented as number of patients (percentage).

*Data are presented as mean ± SD (range).

†Hepatobiliary cancer; ampulla of Vater cancer, common bile duct cancer, and gallbladder cancer.

‡Pancreatic cancer; pancreatic adenocarcinoma and malignant intraductal papillary mucinous neoplasm.

WBC indicates white blood cell.

TABLE 2. Diagnostic Imaging Features on the Per-Lesion Basis

Modality	Sequence	Imaging Features	Abscess (n = 35)	Metastasis (n = 62)	P	
CT	AP	Density			NA	
		Low	35 (100)	52 (83.9)		
		Iso	0	2 (3.2)		
	AP	Rim enhancement	High	0	8 (12.9)	
			Absent	5 (14.3)	15 (24.2)	0.247
	AP	Present	Present	30 (85.7)	47 (75.8)	
			Perilesional enhancement			<0.001†
	AP	Absent	Absent	10 (28.6)	44 (71.0)	
			Present	25 (71.4)	18 (29.0)	
	AP	Patchy enhancement	Absent	8 (22.9)	54 (87.1)	<0.001†
			Present	27 (77.1)	8 (12.9)	
	PP	Density				NA
	PP	Low	Low	35 (100)	35 (100)	
			Margin			0.487
	PP	Well defined	Well defined	10 (28.6)	22 (35.5)	
			Ill defined	25 (71.4)	40 (64.5)	
PP	Rim enhancement	Absent	6 (17.1)	28 (45.2)	0.005†	
		Present	29 (82.9)	34 (54.8)		
PP	Bile duct dilatation	Absent	15 (42.9)	51 (82.3)	<0.001†	
		Present	20 (57.1)	11 (17.7)		
AP, PP	Size discrepancy	Absent	31 (88.6)	57 (91.9)	0.718	
		Present	4 (11.4)	5 (8.1)		
MRI	AP	SI			0.345	
		Low	29 (96.7)	57 (100)		
		High	1 (3.3)	0		
	AP	Rim enhancement	Absent	0	1 (1.6)	>0.999
			Present	35 (100)	61 (98.4)	
	AP	Perilesional enhancement	Absent	7 (20.0)	39 (62.9)	<0.001†
			Present	28 (80.0)	23 (37.1)	
	AP	Patchy enhancement	Absent	12 (34.4)	46 (74.2)	<0.001†
			Present	23 (65.7)	16 (25.8)	
	PP	SI				NA
	PP	Low	Low	35 (100)	62 (100)	
			Rim enhancement			0.481
	PP	Absent	Absent	2 (5.7)	7 (11.3)	
			Present	33 (94.3)	55 (88.7)	
	TP	SI				NA
	TP	Low	Low	35 (100)	62 (100)	
			Rim enhancement			0.046
	TP	Absent	Absent	4 (11.4)	19 (30.6)	
Present			31 (88.6)	43 (69.4)		
HBP	Margin	Well defined	24 (68.6)	61 (98.4)	<0.001†	
		Ill defined	11 (31.4)	1 (1.6)		
HBP	Dark rim				<0.001†	

Continued next page

TABLE 2. (Continued)

Modality	Sequence	Imaging Features	Abscess (n = 35)	Metastasis (n = 62)	P
	HBP	Absent	32 (91.4)	13 (21.0)	<0.001†
		Present	3 (8.6)	49 (79.0)	
	DWI	Perilesional low SI			0.017‡
		Absent	20 (57.1)	58 (93.5)	
		Present	15 (42.9)	4 (6.5)	
		Pattern			
	T1WI, HBP	Rim hyperintensity	12 (34.3)	25 (40.3)	0.002†
		Hyperintensity in the whole lesion	13 (37.1)	36 (58.1)	
		Central hyperintensity	10 (28.6)	1 (1.6)	
	T1WI, T2WI	Size discrepancy			<0.001†
		Absent	29 (82.9)	62 (100)	
		Present	6 (17.1)	0	
		Size discrepancy			<0.001†
		Absent	27 (77.1)	62 (100)	
		Present	8 (22.9)	0	

Data are presented as number of patients (percentage).
 NA indicates not applicable.

DWI, and size discrepancy were significantly more frequent with abscesses than metastases (Table 2). Representative hepatic abscess and metastasis cases are presented in Figures 2 and 3, respectively. The interobserver agreement was excellent for bile duct dilatation and good for rim enhancement in AP of CT, patchy parenchymal enhancement in AP of MRI, rim enhancement in TP, dark rim and perilesional low SI in HBP, and DWI pattern. Moderate interobserver agreements were noted for other parameters.

Risk Factor Analysis for Hepatic Abscess

Univariable GEE regression showed that abnormal segment neutrophils, CRP elevation, and direct bilirubin elevation among

laboratory parameters; perilesional enhancement, patchy parenchymal enhancement, and biliary dilatation among CT parameters; and patchy parenchymal enhancement and absence of dark rim among MRI parameters were associated with hepatic abscess significantly more than metastases (all *P* < 0.05, Table 3).

Comparisons of Diagnostic Performances

The absence of dark rim in HBP showed significantly higher sensitivity (91.4% vs 74.3%–77.1%, *P* ≤ 0.025) and NPV (94.2% vs 84.5%–87.1%, *P* ≤ 0.04) than other parameters. The combination of abnormal segment neutrophil and patchy parenchymal enhancement in AP of CT showed significantly higher

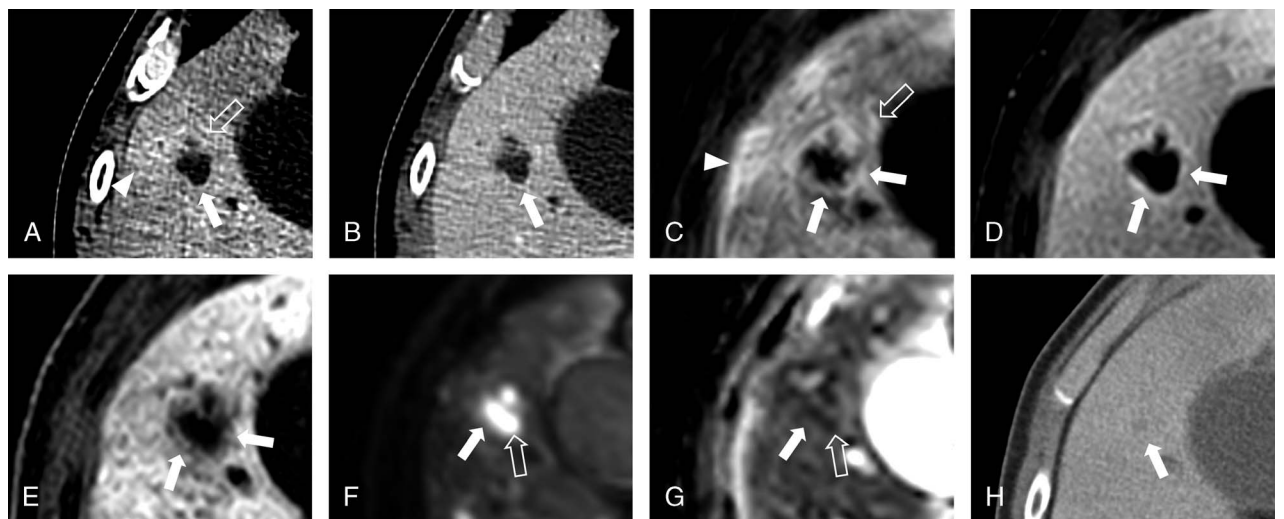


FIGURE 2. A case of hepatic abscess in a 83-year-old male patient with suprapancreatic common bile duct cancer. On CT, a 2.3-cm-sized well-defined focal hepatic lesion was present in the segment V of liver with diffuse bile duct dilatation (not shown). The lesion showed rim enhancement (arrows) on both (A) arterial and (B) portal phases. Also, there were perilesional enhancement (white outlined arrow) and patchy parenchymal enhancement (arrow head) on AP. On MRI, the lesion showed persistent rim enhancement (arrows) from (C) AP to (D) TP. Perilesional enhancement (white outlined arrow) and patchy parenchymal enhancement (arrow head) were also present on AP, and perilesional low SI was not present on hepatobiliary phase (E). Diffusion restriction was noted in the center of the lesion (white outlined arrow), not the periphery (arrow) on (F) b-800 DWI and (G) apparent diffusion coefficient. After 3 months with antibiotics treatment, the lesion markedly decreased size (H), and it was clinically diagnosed as a hepatic abscess.

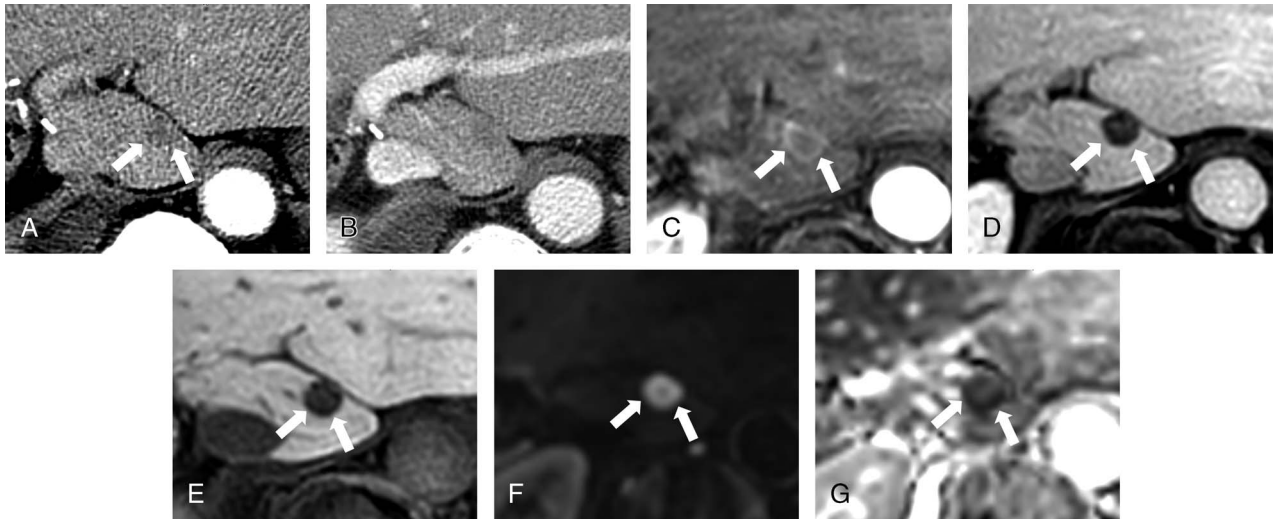


FIGURE 3. A case of hepatic metastasis in a 76-year-old male patient with history of colon cancer operation. On CT, a 1.3-cm-sized well-defined focal hepatic lesion was present in the segment I of liver. The lesion showed rim enhancement on AP (A), not on portal phase (B). There was no perilesional enhancement or patchy parenchymal enhancement on AP. On MRI, the lesion showed persistent rim enhancement from (C) AP to (D) TP. Dark SI rim was noted on hepatobiliary phase (E), and the periphery of the lesion showed diffusion restriction on (F) b-800 DWI and (G) apparent diffusion coefficient. It was confirmed as a hepatic metastasis after the wedge resection surgery.

specificity (95.2% vs 79.0%–87.1%, $P \leq 0.025$) and PPV (89.3% vs. 66.7%–77.1%, $P \leq 0.035$) than each parameter alone. The addition of MRI (absence of dark rim in HBP) to CT (patchy parenchymal enhancement in AP) resulted in significantly higher specificity, PPV, and diagnostic accuracy than CT alone (specificity, 96.8% vs 87.1%; PPV, 93.1% vs 77.1%; diagnostic accuracy, 89.7% vs 83.5%; $P \leq 0.031$) without significant differences of sensitivity and NPV (Table 4).

DISCUSSION

We believe that our study is one of the first to evaluate the efficacy of combined assessment of CT and MRI for the differential

diagnosis between hepatic abscess and metastasis. We found that the combination of CT and MRI imaging features significantly improved the diagnostic performance for the differentiation of hepatic abscess from metastasis compared with CT alone. In the univariate GEE regression, abnormal segmental neutrophil, patchy parenchymal enhancement on CT, and absence of dark rim on MRI were significant parameters differentiating hepatic abscess from metastasis (all $P < 0.01$). The combination of CT and MR findings showed significantly higher specificity, PPV, and diagnostic accuracy than CT alone, without significant differences in sensitivity and NPV.

The improved diagnostic performance might be attributed to the complementary detection of significant imaging features on

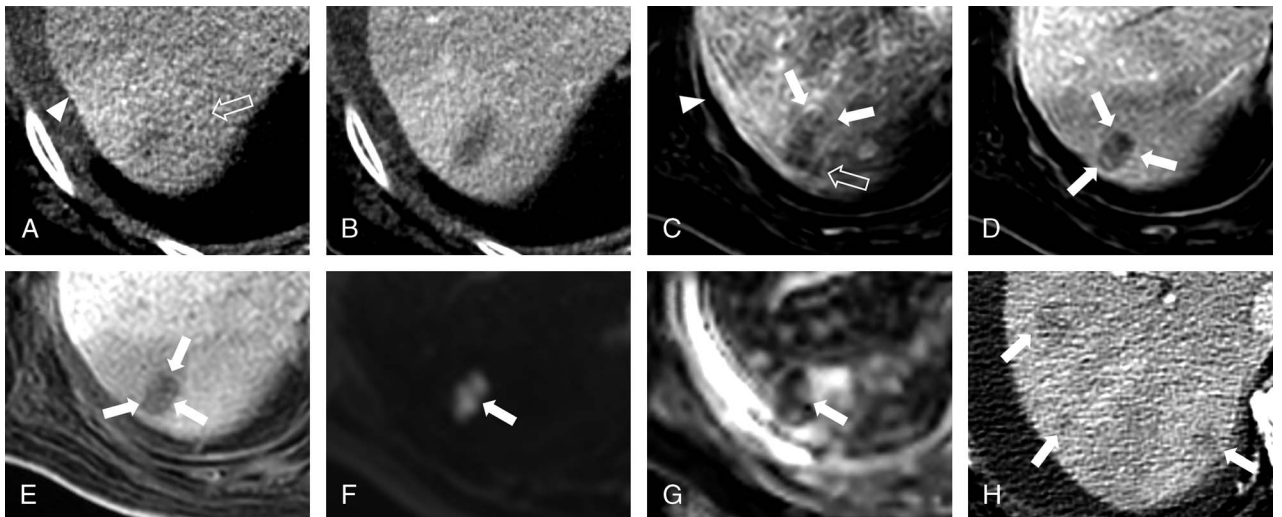


FIGURE 4. An unusual case of hepatic metastasis in a 81-year-old female patient with pancreas head cancer. On CT, a 2.1-cm-sized ill-defined focal hepatic lesion was present in the segment VI of liver with diffuse bile duct dilatation (not shown). The lesion did not show rim enhancement either (A) arterial or (B) portal phase. However, there were perilesional enhancement (white outlined arrow) and patchy parenchymal enhancement (arrowhead) on AP. On MRI, the lesion showed persistent rim enhancement (arrows) from (C) AP to (D) TP. There were perilesional enhancement (white outlined arrow) or patchy parenchymal enhancement (arrowhead) on AP. Dark SI rim was noted on hepatobiliary phase (E), and diffusion restriction was noted in whole lesion on (F) b-800 DWI and (G) apparent diffusion coefficient. After 1-month follow-up (H), the lesion slightly increased, and other new hepatic metastases have developed.

TABLE 3. Univariable GEE Regression Analysis for Differentiation of Hepatic Abscess From Metastasis

Parameters	Univariable Analysis		
	Odds Ratio	95% CI	P
Laboratory findings			
Abnormal WBC	2.078	0.553–7.800	0.279
Abnormal segment neutrophil	9.511	2.095–43.172	0.004
CRP elevation	9.121	1.003–82.947	0.050
Total bilirubin elevation	2.672	0.683–10.456	0.158
Direct bilirubin elevation	6.076	1.437–25.681	0.014
CT			
AP rim enhancement [absence]	1.066	0.904–1.257	0.446
AP perilesional enhancement [absence]	1.201	1.023–1.410	0.026
AP patchy parenchymal enhancement [absence]	27.516	4.370–173.268	<0.001
PP margin [well-defined margin]	0.588	0.263–1.310	0.194
PP rim enhancement [absence]	1.763	0.872–3.562	0.114
Bile duct dilatation [absence]	5.481	1.319–22.767	0.019
Size discrepancy [absence]	0.988	0.896–1.088	0.802
MRI			
AP rim enhancement [absence]	1.086	0.896–1.317	0.401
AP perilesional enhancement [absence]	1.522	0.926–2.499	0.097
AP patchy parenchymal enhancement [absence]	5.330	1.285–22.118	0.021
PP rim enhancement [absence]	1.042	0.890–1.219	0.611
TP rim enhancement [absence]	1.131	0.973–1.316	0.108
HBP margin [well-defined]	0.824	0.336–2.022	0.673
HBP dark rim [presence]	2.927	1.307–6.556	0.009
HBP perilesional low SI [absence]	1.429	0.941–2.169	0.094
DWI pattern			
Rim hyperintensity	1.229	0.611–2.469	0.563
Hyperintensity at the whole lesion	0.668	0.311–1.436	0.302
Central hyperintensity	—	—	—
HBP size discrepancy [absence]	—	—	—
T2 size discrepancy [absence]	—	—	—

The reference category is in square brackets.
95% CI indicates 95% confidence interval.

TABLE 4. Diagnostic Performances of Laboratory and Imaging Findings for Differentiation of Hepatic Abscess From Metastasis

	Sensitivity	Specificity	PPV	NPV	Diagnostic Accuracy
Abnormal segment neutrophil (1)	74.3 (26/35)	79.0 (49/62)	66.7 (26/39)	84.5 (49/58)	77.3 (75/97)
Patchy parenchymal enhancement on CT (2)	77.1 (27/35)	87.1 (54/62)	77.1 (27/35)	87.1 (54/62)	83.5 (81/97)
Absence of dark rim in HBP (3)	91.4 (32/35)	79.0 (49/62)	71.1 (32/45)	94.2 (49/52)	83.5 (81/97)
(1) and (2)	71.4 (25/35)	95.2 (59/62)	89.3 (25/28)	85.5 (59/69)	86.6 (84/97)
(2) and (3)	77.1 (27/35)	96.8 (60/62)	93.1 (27/29)	88.2 (60/68)	89.7 (87/97)
(1) vs. (2)*	0.564	0.197	0.173	0.335	0.238
(1) vs. (3)*	0.014†	>0.99	0.543	0.016†	0.308
(2) vs. (3)*	0.025†	0.225	0.434	0.040†	>0.99
(1) vs. (1) and (2)*	0.317	0.002†	0.002†	0.527	0.012†
(2) vs. (1) and (2)*	0.157	0.025†	0.035†	0.397	0.453
(2) vs. (2) and (3)*	>0.99	0.014†	0.014†	0.064	0.031†
(3) vs. (2) and (3)*	0.025†	0.001†	0.002†	0.059	0.210

Data are presented as percentage (number) of each parameter.
*P values of each comparison.
†P value of <0.05.

CT and MRI. Iodine contrast-enhanced CT could complement weak contrast enhancement on gadoteric acid-enhanced MRI, and the low lesion-to-liver contrast on CT could be supplemented by MRI.⁹ Furthermore, the unique HBP of MRI with a hepatobiliary agent might assist in the characterization of focal hepatic lesions.^{10,11} When indeterminate hepatic lesions are found on CT, MRI is performed for further characterization in our daily clinical practice. The accuracy of the combined assessment of CT and MRI for differentiating hepatic abscess from metastasis in our study was 89.7%, which was higher than that of the previous literatures: 78.9% to 83.5% CT alone and 72.2% to 88.9% MRI alone.^{1,4} Our study supports that diagnostic performance is improved in the differentiating hepatic abscess and metastasis when, in real-world workflows, the results of both imaging modalities are used together to differentiate these possibilities.

We only included focal hepatic lesions ≤ 3 cm on both CT and MRI. Larger hepatic lesions are more likely to show the typical imaging features of hepatic abscesses, such as targetoid appearance or cluster signs.¹² In such cases, the differential diagnosis between hepatic abscess and metastasis might not be challenging, making the yield of MRI addition low. Furthermore, larger hepatic lesions are easier to access in the image-guided biopsy. Therefore, the results of our study, which only included small hepatic lesions, would be more clinically helpful in challenging cases with small lesion size or overlapping imaging features between hepatic abscess and metastasis. Furthermore, the interobserver agreements for AP patchy parenchymal enhancement on CT and dark rim in HBP were moderate to good, which might make our studied imaging features clinically applicable.

Focal or segmental patchy parenchymal enhancement of the liver in AP is caused by inflammatory cell infiltration and stenosis of portal venules within portal tracts surrounding hepatic abscesses and compensatory arterial flow increase.¹³ It can be associated with various diseases other than hepatic abscesses, such as arteriportal shunt, portal vein compression or thrombosis, and aberrant blood supply.^{14,15} The wedge-shaped enhancement mimicking nontumorous arteriportal shunt on CT and MRI is a frequent imaging feature of hepatic metastasis by pancreatic adenocarcinoma.¹⁶ However, it is more common in hepatic abscesses than in metastasis.^{1,17} Similarly, the incidence of AP patchy parenchymal enhancement on CT and MRI was significantly higher in hepatic abscess than in metastasis, and it was the only independent parameter associated with a hepatic abscess in the multivariable analysis of CT (Fig. 4).

The dark rim in HBP imaging is a reported imaging feature of hepatic metastasis. It reflects the transitory perfusion within the well-vascularized peripheral portion of the hepatic metastasis with abundant tumor cellularity.^{3,18} On the contrary, the periphery of the hepatic abscess shows retention of the contrast agent owing to extensive fibrous tissues and inflammatory changes relative to the necrotic central portion, which makes the periphery of the hepatic abscess appear as a “nondefect (isointensity to hyperintensity)” in HBP.^{3,19,20} Thus, these different histopathological processes might result in different appearances of the periphery of the hepatic abscess and metastasis in HBP.

Previous studies suggested that persistent rim enhancement on the dynamic scan was a significant imaging parameter for differentiating hepatic abscess from metastasis,^{1,4} although our study did not evaluate this. However, our study also showed that the rate of PP rim enhancement on CT and TP rim enhancement on MRI was significantly higher in hepatic abscess than in metastasis. These findings may also help to distinguish between the 2 lesions, although these features were not included in our GEE analysis. The rate of AP rim enhancement on CT and MRI was high in both diseases, which did not help to differentiate between them. The size discrepancy on MRI showed a significant difference between

the 2 lesions and was not found in the metastasis; however, the frequency of size discrepancy was lower (17.1%–22.9%) in hepatic abscess than the finding of a previous study.⁴ This may be because the definition of the size discrepancy was applied more strictly in this study; the size of the lesion on unenhanced T1WI was less than 3 mm and less than 30% compared with the lesion in T2WI or HBP.

Among the laboratory parameters, the abnormal segment neutrophil percentage was significantly different between hepatic abscess and metastasis. Eleven of 16 patients with hepatic abscess (68.8%) showed abnormal segment neutrophils. It showed moderate sensitivity and specificity for the differentiation of hepatic abscess from metastasis. Inflammation by small hepatic abscess might not always be enough to cause abnormal segmental neutrophil on a laboratory test. The differential diagnosis between 2 diseases with only clinical symptoms and laboratory findings is challenging, necessitating imaging studies, including CT and MRI.

There are some limitations to our study. First, the number of patients with hepatic abscess and metastasis evaluated in this study was small. One of the reasons was the strict inclusion criteria of including patients whose CT and MRI were performed within only 4 days of one another and that we also excluded several patients when lesion size exceeded 3 cm. Future studies with a larger number of patients would strengthen our results. Second, only 14.3% of hepatic abscess and 32.3% of metastasis were histopathologically confirmed. However, a biopsy of small hepatic lesions is difficult in many cases. Finally, we did not unify the types of preexisting malignancy. Patients with pancreaticobiliary cancer are more prone to develop both hepatic abscess and metastasis. Therefore, the differential diagnosis between the 2 diseases would be more challenging. However, the number of patients with pancreaticobiliary cancer was too small to unify the preexisting malignancy or perform subgroup analysis.

In conclusion, the combination of CT and MRI imaging features significantly improved the diagnostic performance for the differentiation of small hepatic abscess from metastasis than CT alone. Therefore, the combined assessment of CT and MRI can be complementary and clinically useful for the differential diagnosis of small hepatic abscess and metastasis.

REFERENCES

- Oh JG, Choi SY, Lee MH, et al. Differentiation of hepatic abscess from metastasis on contrast-enhanced dynamic computed tomography in patients with a history of extrahepatic malignancy: emphasis on dynamic change of arterial rim enhancement. *Abdom Radiol (NY)*. 2019;44:529–538.
- Eun HW, Kim JH, Hong SS, et al. Malignant versus benign hepatic masses in patients with recurrent pyogenic cholangitis: MR differential diagnosis. *Abdom Imaging*. 2012;37:767–774.
- Choi SH, Lee CH, Kim BH, et al. “Nondefect” of arterial enhancing rim on hepatobiliary phase in 3.0-T gadolinium-ethoxybenzyl-diethylenetriamine pentaacetic acid-enhanced liver magnetic resonance imaging: distinguishing hepatic abscess from metastasis. *J Comput Assist Tomogr*. 2013;37:849–855.
- Choi SY, Kim YK, Min JH, et al. The value of gadoteric acid-enhanced MRI for differentiation between hepatic microabscesses and metastases in patients with periampullary cancer. *Eur Radiol*. 2017;27:4383–4393.
- Jeffrey RB Jr, Tolentino CS, Chang FC, et al. CT of small pyogenic hepatic abscesses: the cluster sign. *AJR Am J Roentgenol*. 1988;151:487–489.
- Balci NC, Semelka RC, Noone TC, et al. Pyogenic hepatic abscesses: MRI findings on T1- and T2-weighted and serial gadolinium-enhanced gradient-echo images. *J Magn Reson Imaging*. 1999;9:285–290.
- Park HJ, Kim SH, Jang KM, et al. Differentiating hepatic abscess from malignant mimickers: value of diffusion-weighted imaging with an emphasis on the periphery of the lesion. *J Magn Reson Imaging*. 2013;38:1333–1341.

8. Tan GJ, Berlangieri SU, Lee ST, et al. FDG PET/CT in the liver: lesions mimicking malignancies. *Abdom Imaging*. 2014;39:187–195.
9. Basha MAA, AlAzzazy MZ, Ahmed AF, et al. Does a combined CT and MRI protocol enhance the diagnostic efficacy of LI-RADS in the categorization of hepatic observations? A prospective comparative study. *Eur Radiol*. 2018;28:2592–2603.
10. Haimerl M, Wachtler M, Platzek I, et al. Added value of Gd-EOB-DTPA-enhanced hepatobiliary phase MR imaging in evaluation of focal solid hepatic lesions. *BMC Med Imaging*. 2013;13:41.
11. Ahn SS, Kim MJ, Lim JS, et al. Added value of gadoxetic acid-enhanced hepatobiliary phase MR imaging in the diagnosis of hepatocellular carcinoma. *Radiology*. 2010;255:459–466.
12. Vilgrain V, Esvan M, Ronot M, et al. A meta-analysis of diffusion-weighted and gadoxetic acid-enhanced MR imaging for the detection of liver metastases. *Eur Radiol*. 2016;26:4595–4615.
13. Mathieu D, Vasile N, Fagniez PL, et al. Dynamic CT features of hepatic abscesses. *Radiology*. 1985;154:749–752.
14. Pradella S, Centi N, La Villa G, et al. Transient hepatic attenuation difference (THAD) in biliary duct disease. *Abdom Imaging*. 2009;34:626–633.
15. Lin G, Lunderquist A, Hagerstrand I, et al. Postmortem examination of the blood supply and vascular pattern of small liver metastases in man. *Surgery*. 1984;96:517–526.
16. Gabata T, Matsui O, Terayama N, et al. Imaging diagnosis of hepatic metastases of pancreatic carcinomas: significance of transient wedge-shaped contrast enhancement mimicking arteriportal shunt. *Abdom Imaging*. 2008;33:437–443.
17. Gabata T, Kadoya M, Matsui O, et al. Dynamic CT of hepatic abscesses: significance of transient segmental enhancement. *AJR Am J Roentgenol*. 2001;176:675–679.
18. Ha S, Lee CH, Kim BH, et al. Paradoxical uptake of Gd-EOB-DTPA on the hepatobiliary phase in the evaluation of hepatic metastasis from breast cancer: is the “target sign” a common finding? *Magn Reson Imaging*. 2012;30:1083–1090.
19. Schneider G, Fries P, Samaras P, et al. Inflammatory pseudotumor of the liver in a patient with congenital granulocytopenia and HCV infection. *Eur J Radiol*. 2003;48:293–298.
20. Runge VM, Wells JW, Williams NM. Hepatic abscesses. Magnetic resonance imaging findings using gadolinium-BOPTA. *Invest Radiol*. 1996;31:781–788.